Detection of Isolated Track Defects Using Axle Box Acceleration from Multibody Simulation and Recurrent Neural Network

Kritat Plodphai, Thitiwut Petcharat, Songsak Suthasupradit and Rattapoohm Parichatprecha *

Department of Civil Engineering, School of Engineering, King Mongkut's Institute of Technology Ladkrabang, Lat Krabang, Lat Krabang, Bangkok 10520, Thailand

***Corresponding Author E-mail:** rattapoohm.pa@kmitl.ac.th

Received: Oct 21, 2025; **Revised:** Jan 06, 2026; **Accepted:** Jan 08, 2026

Abstract

Railway track inspection is typically conducted cyclically, which is slow, budget-intensive, and time-consuming, as it can only be performed during non-service periods when trains are not in operation. Currently, there are emerging concepts and research studies utilizing railway defect detection through acceleration measurements from axle box mounted on service trains, as this approach offers easier implementation, reduced costs, and time efficiency compared to conventional methods. However, the diagnostic process remains challenging due to the high complexity and large volume of data involved. This research presents a method for applying Recurrent Neural Network (RNN) that works with time-series data in diagnosing railway defects by classifying three specific types of isolated defects: squats and corrugation. The training samples for the neural network were derived from axle box acceleration data obtained through multibody simulation analysis that modeled various railway conditions, speeds, and defect characteristics. A total of 360 samples from the multibody model were used for training, validation, and testing. The study results showed that the Recurrent Neural Network (RNN) achieved an average defects classification accuracy of 91.67%. Furthermore, the study findings revealed that the developed RNN model can accurately predict the location and classify defects, with particularly high accuracy in predicting the location and defects caused by long-pitch corrugation. The study concluded that the developed RNN model can efficiently learn and classify defects from axle box acceleration data obtained from multibody simulation. This approach can be applied as a guideline for railway damage diagnosis in future maintenance applications.

Keywords: Recurrent Neural Network (RNN), Rail Squats, Rail Corrugation, Axle Box Acceleration, Multibody Simulation

1. Introduction

Railway inspection and maintenance typically rely on visual inspection methods conducted through walking surveys along railway tracks with portable inspection equipment. However, this approach is inherently limited; it is incapable of detecting internal damage, such as dynamic defects, which are not visually apparent. Furthermore, this method is resource-intensive, necessitating significant time and manpower to monitor extensive railway networks [1]. Alternatively, track recording vehicles are employed to measure parameters including track level and alignment, track gauge, rail twist, curvature and curve radius, gradient, and track position via integrated GPS and displacement sensors [2]. While this method provides accurate inspection results, it involves very high operational costs and can only be performed during rest periods.

Indirect railway condition monitoring has received significant attention in recent years [3] driven by advancements in sensing and computational technologies that have created new approaches for improving and developing accurate and cost-effective track condition monitoring systems. This involves installing sensors that measure dynamic responses, typically mounted on train components near the rails, such as at the axle box. This method enables the installation of measuring instruments on multiple passenger trains and allows for continuous monitoring of railway track conditions. Signal processing techniques on stress-based methods are widely used due to their low cost, high accuracy, and ease of installation [4]. To ensure comprehensive detection of damage occurrences, analysis is requisite to determine the optimal sampling rate and sensor frequency [5].

Elevated load capacities and augmented operational speeds contribute to heightened stress levels at the wheel-rail interface, a condition further exacerbated by existing track degradation [6–9]. Isolated track defects typically have wavelengths less than 2 m; these include corrugation, squats, rail joints, and rail welds [10–17]—induce substantial dynamic impact forces. These forces accelerate rail deterioration, which may subsequently evolve into critical failures, including fatigue cracks or structural damage to the railway infrastructure [18]. To prevent such occurrences, early-stage detection and monitoring are imperative to maintain infrastructural integrity.

Simulation-based dynamic response analysis has been validated to yield results consistent with field measurements [18], by refining the defect geometry to represent a loaded condition—particularly by modeling the squat as a parabolic shape to account for

crack closure under wheel load—and by optimizing the lateral wheel-rail contact position. Such simulation approaches are extensively utilized in applications such as estimating vehicle-structure clearance [19]. Specifically, axle box dynamic responses are increasingly integrated with other parameters for maintenance frameworks; notably, these include the refinement of track quality indices (TQI) for status assessment [20] and the incorporation of artificial intelligence (AI) [21]. Within railway systems, these AI-drive applications span multiple sub-disciplines, including inspection and maintenance, traffic planning and management, safety operations, signaling and control, and passenger demand forecasting, with inspection and maintenance constituting the largest proportion. A primary advantage of this approach lies in its ability to elucidate the correlations between influential factors and damage occurring on railway tracks [22], thereby supporting informed decision-making for optimized infrastructure monitoring.

Neural networks (NNs) represent a prevalent machine learning paradigm for predictive modeling based on training data. A typical structure consists of three parts: the input layer, facilitating data entry; the hidden layer, responsible for pattern extraction; and the output layer, which yields the final predictions. NNs have been deployed to detect soil stiffness degradation by analyzing axle box acceleration anomalies relative to healthy track baselines. Sensitivity analyses further indicate that these models maintain robustness in identifying multiple defects despite noise interference [23]. Furthermore, Recurrent Neural Networks (RNNs)—distinguished by their efficacy in processing sequential or time-series data—have been implemented to classify defect types by correlating vertical acceleration signals with specific damage patterns in scaled vehicle-track models [24]. However, previous studies remain somewhat limited in representing multiple defect locations or in using vertical acceleration values derived from the scaled model simulations as training data for the model.

This research utilizes dynamic response analysis to simulate the vibrational behavior of various train components using a multibody model in Universal Mechanism Version 9.1.3 software. Vertical acceleration signals from the axle box are segmented, labeled at defect sites, and integrated into a Recurrent Neural Network (RNN) framework for classification. The results demonstrate that the network accurately categorizes types and localizes both discrete and wavelength-based track defects. This study proposes a robust, non-invasive methodology for indirect track monitoring—one that maintains operational continuity while enhancing maintenance efficiency and cost-effectiveness.

2. Train-Track Model

2.1 Train Multibody Model

This study employs the multibody model of the Manchester Benchmark Vehicle 1 [25] as shown in **Figure 1**, derived from the standard ERRI B176 passenger coach. This specific configuration is simplified to minimize computational, characterized as a vehicle without a yaw damper system and with reduced complexity, featuring a simple primary suspension system, symmetric car body, and non-tilting suspension with simple damping rates. Such simplification facilitates the efficient simulation of dynamic responses specifically induced by track defects. The masses of the wheelset, bogie, and car body are 1,813 kg, 2,615 kg, and 32,000 kg, respectively. The dimensional specifications of the railway vehicle and suspension system characteristics are presented in **Table 1** and **Table 2**, respectively. The connection point between the bogie and car body is illustrated in **Figure 2**, and the wheel contact surface profile follows the S1002 profile [25], as shown in **Figure 3** from Universal Mechanism software.

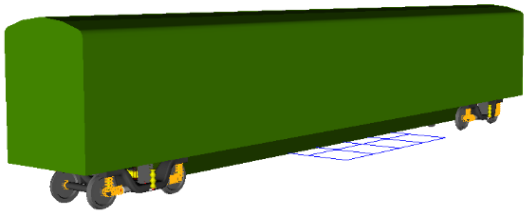

Figure 1 Manchester Benchmark Vehicle 1

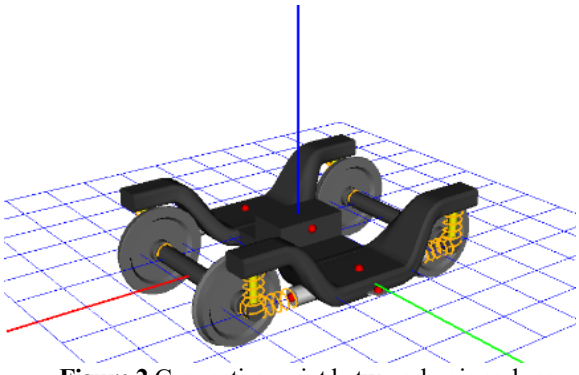

Figure 2 Connection point between bogie and car body

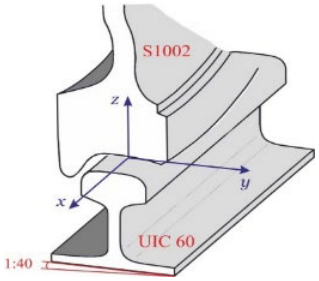

Figure 3 Wheel S1002 profile

Table 1 Vehicle Dimensions

Variables	Values
Bogie semi pivot spacing (mm)	9500
Bogie semi wheelbase (mm)	1280
Wheel radius (mm)	460
Height above rail level of bogie cg (mm)	600
Height above rail level of body cg (mm)	1800

Table 2 Suspension Characteristics

Variables	Values
Primary suspension stiffness (kN/m)	1220
Secondary suspension stiffness (kN/m)	430
Secondary roll bar stiffness (kNm/rad)	940
Secondary traction rod stiffness (kN/m)	5000

2.2 Track Properties

Standard UIC 60 railway tracks with a track gauge of 1.435 m are adopted in this study. A straight track section with a length of 100 m is considered, assuming a rigid track foundation. Under this assumption, the rails are treated as non-deformable and remain stationary when subjected to forces induced by the railway wheels. This simplification is introduced to minimize the influence of ballast-induced noise, thereby enabling a comprehensible investigation of the dynamic responses primarily associated with the simulated track defects. while still adequately capturing the effects of track surface irregularities. For track surface irregularities, values according to FRA standards are used, with random addition of three types of isolated track defects: short-, medium-, and long-wavelength defects, totaling five defect locations.

2.2.1 The FRA PSD Standards

The Federal Railroad Administration (FRA) [26] of the United States classifies railway tracks into 9 classes, where Classes 1 through 6 are designed for conventional railways, and Classes 7 through 9 are designed for high-speed rail. For each track class, random track irregularities are described using the One-sided Power Spectral Density (PSD) function. Additionally, due to limitations of track irregularity measuring equipment, this PSD function is only applicable within the wavelength range of 1.524 m to 304.8 m. The empirical formulas for PSD are presented in Eqs. (1)–(2).

$$S_{av}(\Omega) = \frac{k \cdot A_v \cdot {\Omega_c}^2}{\Omega^2 \cdot (\Omega^2 + {\Omega_c}^2)} \quad (1)$$

$$S_{al}(\Omega) = \frac{k \cdot A_a \cdot {\Omega_c}^2}{\Omega^2 \cdot (\Omega^2 + {\Omega_c}^2)} \quad (2)$$

Where:
$S_{av}(\Omega)$ is the PSD of vertical track irregularities
$S_{al}(\Omega)$ is the PSD of horizontal track irregularities
Ω is spatial wavenumber
Ω_c is critical wavenumber
A_v, A_a is roughness coefficient
k is constant approximately 0.25

The wave number is related to the frequency per unit time f_h (Hertz) by the relationship $\Omega = 2\pi f_h / V$ and the parameters used for Eqs (1)–(2) are given in **Table 3**.

Table 3 Coefficients for Power Spectral Density [26]

Line Grade	A_v	A_a	Ω_c
1	1.2107	3.3634	0.8245
2	1.0181	1.2107	0.8245
3	0.6816	0.4128	0.8245
4	0.5376	0.3027	0.8245
5	0.2095	0.0762	0.8245
6	0.0339	0.0339	0.8245

2.2.2 PSD-to-Track Irregularities Transformation

In this research, the PSD Standard is defined as a function of wave number (rad/m). Random track irregularities can be generated using trigonometric series as shown in Eq. (3).

$$r(x) = \sqrt{2} \sum_{n=0}^{N-1} A_n \cos(\Omega_n \cdot x + \theta_n) \quad (3)$$

Where:
N is number of angular wave numbers considered
Ω_n is discrete angular wave number, given by Eq. (4).

$$\Omega_n = n \cdot \Delta\Omega = n \cdot \frac{\Omega_u - \Omega_l}{N}, \quad n = 1,2,\dots N-1 \quad (4)$$

Where:
Ω_u and Ω_l are the upper and lower bounds used for consideration.
θ_n is the phase angle randomly distributed between 0 and 2π.
A_n is random series amplitude coefficients
G_{rr} is the PSD standard, defined as Eq. (5)

$$A_0 = 0,$$
$$A_1 = \sqrt{\left(\frac{1}{2\pi} \cdot G_{rr}(\Delta\Omega) + \frac{4}{12\pi} \cdot G_{rr}(0)\right) \cdot \Delta\Omega},$$
$$A_2 = \sqrt{\left(\frac{1}{2\pi} \cdot G_{rr}(2\Delta\Omega) + \frac{4}{12\pi} \cdot G_{rr}(0)\right) \cdot \Delta\Omega}, \quad (5)$$
$$A_n = \sqrt{\left(\frac{1}{2\pi} \cdot G_{rr}(\Omega_n)\right) \cdot \Delta\Omega},$$
$$\text{for } n = 3,4,\dots N-1$$

2.3 Track Damage

Railway track defects with different wavelengths require repair using distinct techniques and methods. Classification of defects based on wavelength is therefore an appropriate criterion. Initially, defects can be classified into two main groups: defects arising from the loss of vertical geometric profile of rails, which typically have wavelengths greater than 2 m, and defects related to corrugation or isolated track defects, which result from material loss at the rail head top surface while the rail level remains intact. The classification of vertical railway track defects in this study follows the standard proposed by Administrador

de Infraestructuras Ferroviarias (Adif) as reported in [5]. According to this classification, rail corrugation and isolated track defects are categorized based on their wavelength into very short (0.03–0.06 m), short (0.06–0.25 m), medium (0.25–0.60 m), and long (0.60–2 m) wavelength ranges, while vertical track alignment defects are classified into short (2–25 m), medium (25–70 m), and long (70–120 m) wavelength ranges.

In this research, the simulation focuses on rail corrugation and isolated track defects, which are further grouped into short-, medium-, and long-wavelength ranges following the above standard [5]. The defect locations are randomly distributed with a total of five positions. The depth of defects is set to 15-30 mm. For isolated defects, the defect width is defined as 200 mm for short-wavelength defects, 400-600 mm for medium-wavelength defects, and 1,500-1,700 mm for long-wavelength defects. Each wavelength range is generated using Eqs. (6)–(7).
For short wavelengths

$$f(x) = d \cdot \left(1 \pm cos\left(\frac{\pi x}{L}\right)\right) \quad (6)$$

For medium and long wavelengths

$$f(x) = \frac{d}{2} \cdot \left(1 - cos\left(\frac{2\pi x}{L}\right)\right) \quad (7)$$

Where:
$f(x)$ is shape function of the track defect
x is current position of the track
d is depth of defect
L is width of defect

2.4 Parametric Studies

Dynamic behavior simulation of the vehicle involves varying parameters according to key factors, namely speed and track irregularities. The speeds used in this research are on straight track at 20, 40, 60, 80, 100, and 120 km/h. For track irregularities, the UIC 60 rail profile is employed, based on FRA standards, which are divided into Classes 1 through 6, with random addition of isolated track defects. Classification by wavelength size is considered, comprising short-, medium-, and long-wavelength ranges, with randomly distributed positions totaling five locations, as shown in **Figures 4–9**.

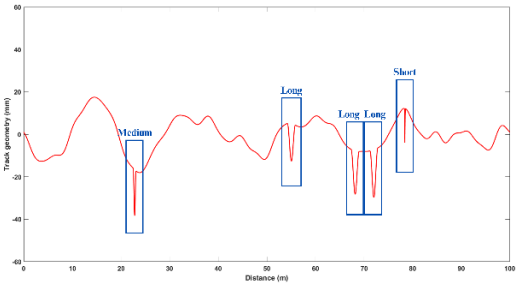

Figure 4 Vertical track irregularities class 1 with isolated track defects

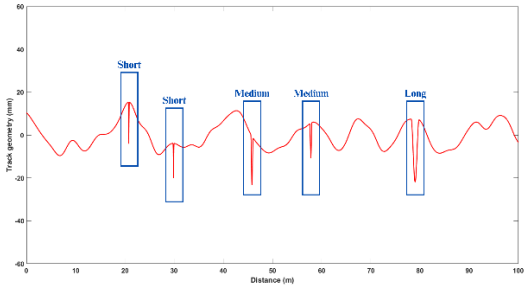

Figure 5 Vertical track irregularities class 2 with isolated track defects

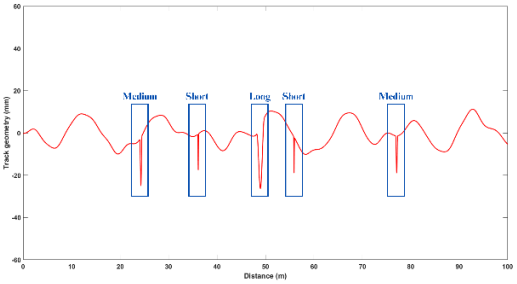

Figure 6 Vertical track irregularities class 3 with isolated track defects

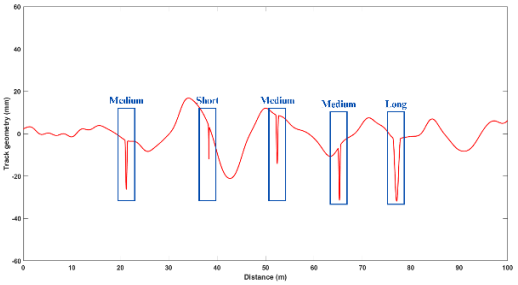

Figure 7 Vertical track irregularities class 4 with isolated track defects

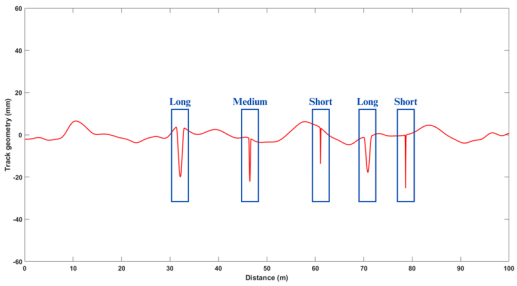

Figure 8 Vertical track irregularities class 5 with isolated track defects

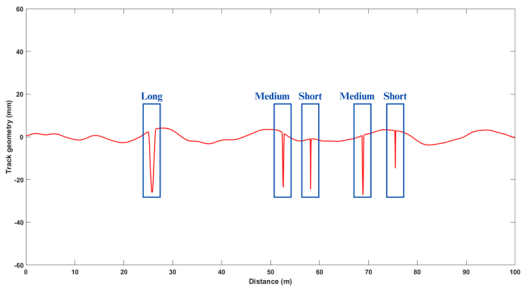

Figure 9 Vertical track irregularities class 6 with isolated track defects

3. Recurrent Neural Network (RNN)

The proposed railway inspection method consists of a first part that utilizes dynamic response analysis results of the train (axle box vertical acceleration) with track irregularities according to FRA Class 1 through 6 and random addition of defects, including short-, medium-, and long-wavelength defects, totaling five locations per route, comprising straight track sections of 100 m over 60 routes. This is followed by labeling the defect types within signal segments to serve as input data for the RNN for predicting the types of defects occurring. The data is divided into three parts: a training dataset to enable the model to learn patterns in the data, a validation dataset to monitor model performance during training and assist in adjusting relevant parameters, and a testing dataset to evaluate the final model's capability with previously unseen new data to measure actual accuracy in practical application.

3.1 Dynamic Response Input

The vertical acceleration signal of the train at the axle box displayed on the Signal Labeler app in the time domain, with a sampling frequency of 2,500 Hz, as shown in **Figures 10–15**, indicates that the signal amplitude level in defect regions increases with higher train speeds. At speeds greater than 100 km/ h, the amplitudes of all three defect types exhibit similar values and characteristics, as shown in **Figures 14–15**.

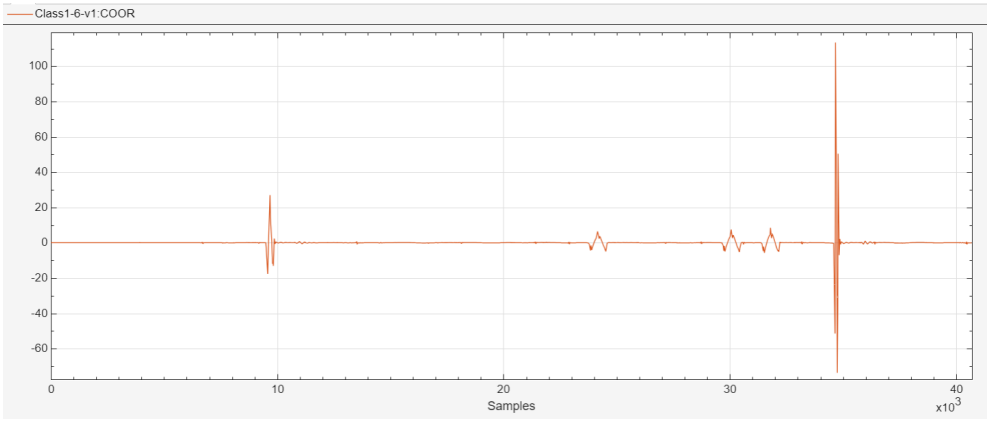

Figure 10 Acceleration signal of class 1 track at 20 km/h displayed on Signal Labeler

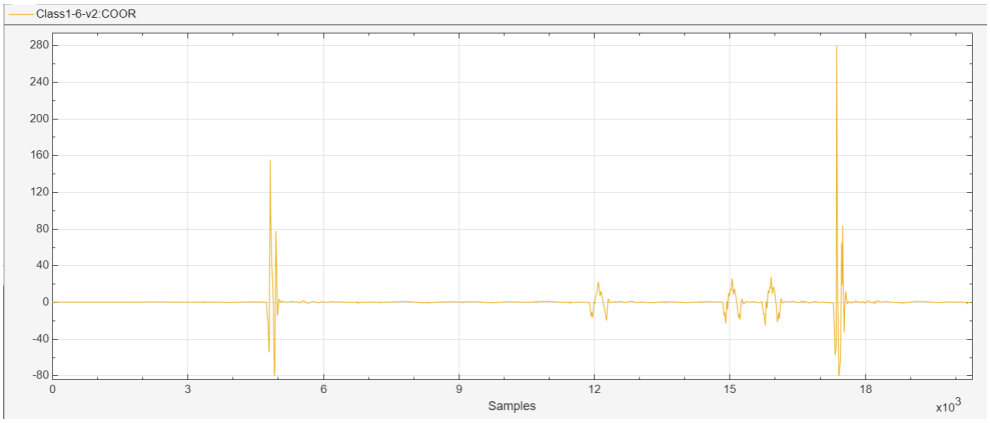

Figure 11 Acceleration signal of class 1 track at 40 km/h displayed on Signal Labeler

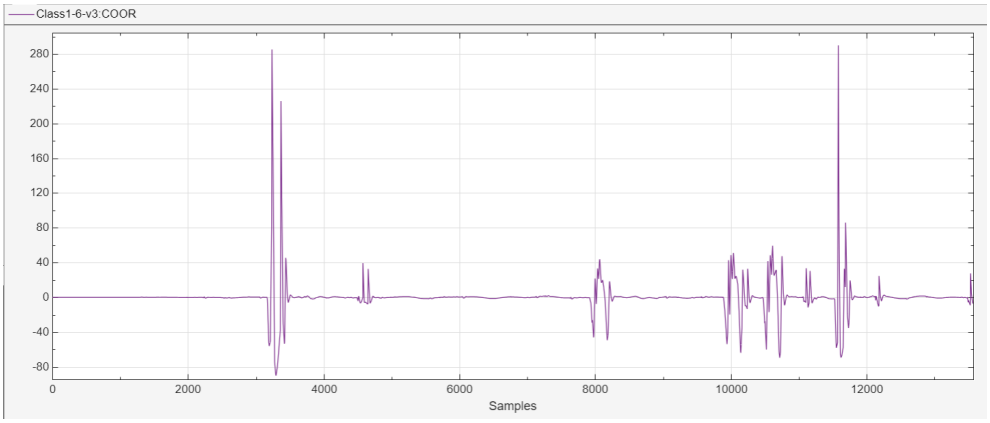

Figure 12 Acceleration signal of class 1 track at 60 km/h displayed on Signal Labeler

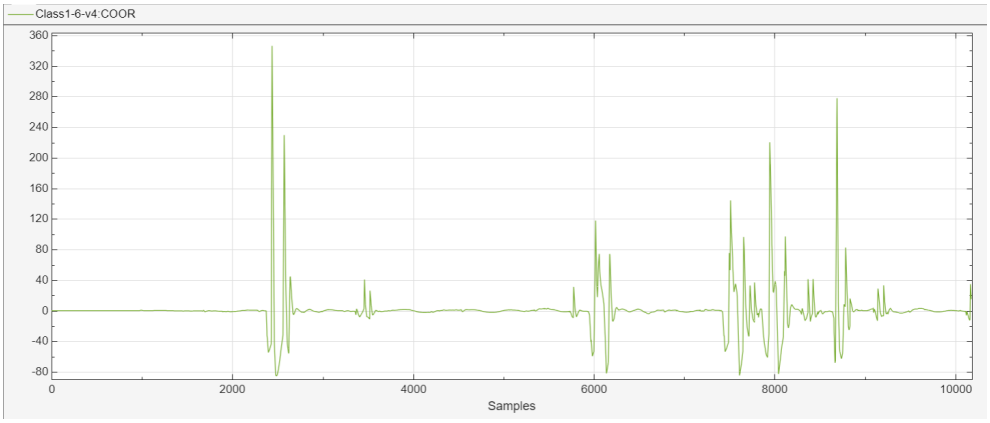

Figure 13 Acceleration signal of class 1 track at 80 km/h displayed on Signal Labeler

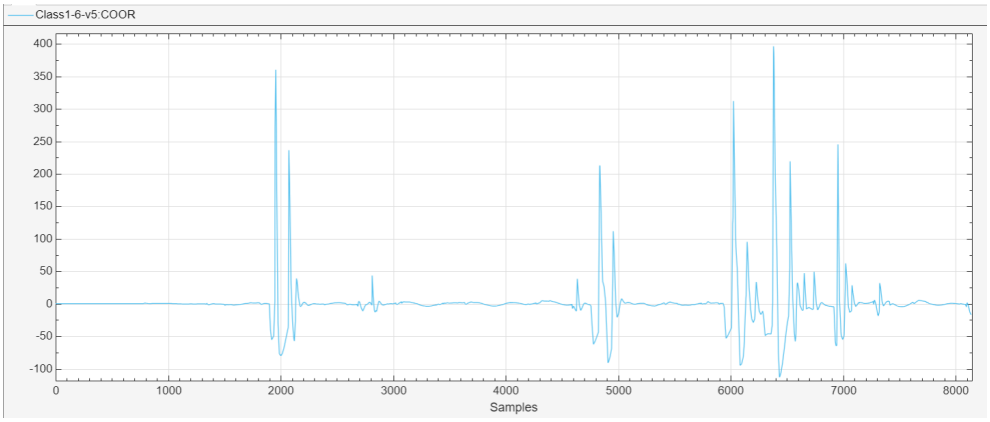

Figure 14 Acceleration signal of class 1 track at 100 km/h displayed on Signal Labeler

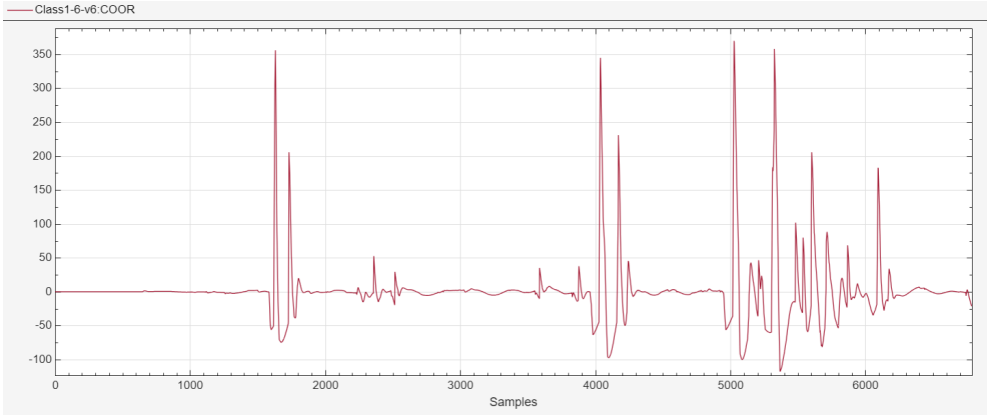

Figure 15 Acceleration signal of class 1 track at 120 km/h displayed on Signal Labeler

3.2 Defect Classification Dataset

Preparing the defect classification dataset is a critical step for collecting data to be used in training and testing the RNN for railway track defect classification. The Signal Labeler app in MATLAB software is used to identify rail defect types by labeling signal segments at defect locations, as shown in the example in **Figure 16**. Subsequently, coordinating data of all defect locations from the entire dataset are stored, as illustrated in **Table 4**. These coordinate values are then used to compile a dataset for training and testing the RNN.

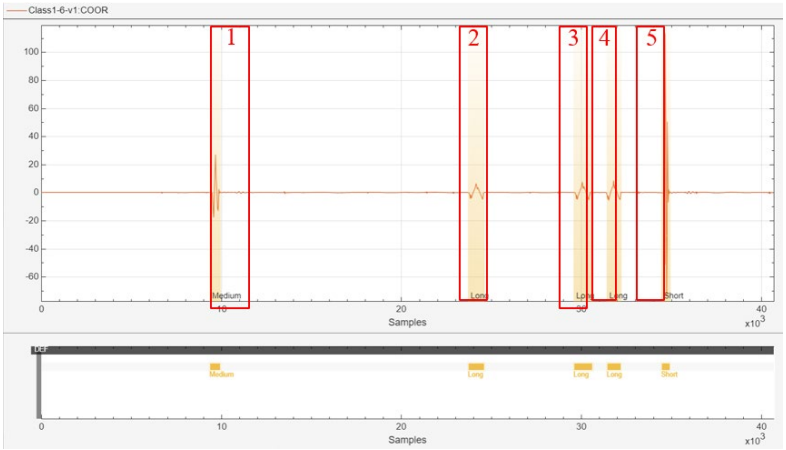

Figure 16 Signal after defect location labeling

Table 4 Coordinated data collect from the Signal Labeler app

Locations	Range		Defect type
1	9399	10019	Medium
2	23706	24631	Long
3	29580	30624	Long
4	31370	32294	Long
5	34471	34978	Short

3.3 Neural Network Training

This step involves training the railway track defect detection system to learn and understand the characteristics of various defect types in the form of dynamic response data with labeled segments identifying different defect types in signal intervals, and employing a RNN for classification, with details as follows:

3.3.1 RNN

Recurrent neural networks are designed to perform effectively with time-series data, where the network output, once generated, is copied and fed back into the network as input. When making decisions, the model not only analyzes the current input and output but also considers previous inputs, these data operate in an interdependent manner. Due to the limitations of conventional RNN with long sequences, another type of RNN was developed: Long Short-Term Memory (LSTM), which addresses this limitation through memory units that can determine when data should be written, read, or forgotten. This enables the model to better capture data relationships within the network [24].

3.3.2 Structure of RNN

The neural network is divided into three parts: the input layer, hidden layer, and output layer, as shown in **Figure 17**. The input layer introduces data into the neural network. In this research, two input values are used: the dynamic response signal value and the train speed value at the same position, totaling 60 routes. Meanwhile, the hidden layer learns patterns in the data. The name "hidden layer" derives from the fact that values calculated in this layer are not displayed as output data. The hidden layer connects to the input layer and output layer through an activation function, comprising "weights" and "bias," as shown in Eq. (8). These weights are adjusted during the training phase. For this research, 100 hidden layer units are selected based on the experience reported in [24], providing a good trade-off between model capacity and generalization performance. The final layer is the output layer, which displays the prediction results, namely the three types of isolated track defects.

$$f(x_1, x_2) = b + w_1 x_1 + w_2 x_2 \tag{8}$$

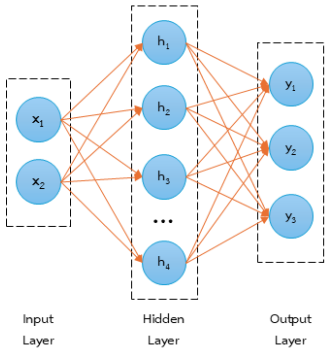

Figure 17 Schematic diagram of RNN

3.3.3 Splitting of dataset

This involves utilizing a labeled dynamic response signal dataset consisting of 360 sets, providing sufficient coverage of the operating conditions considered. The dataset is divided into three parts: a training dataset, a validation dataset, and a testing dataset for the railway track defect detection system. The details of the dataset split ratios are shown in **Table 5**. The dataset is randomly shuffled at the sequence level and then split according to the specified ratios.

Table 5 Dataset split details

Dataset	Ratio	Volume
Training	0.8	288
Validation	0.1	36
Testing	0.1	36

3.3.4 Defining variables

To enable efficient classification of track defects, which is a critical component for allowing the network to appropriately learn hidden patterns in the data, the layers and various parameters of the RNN have been configured, with details shown in **Table 6** and **Table 7**.

Table 6 Neural Network layer

Layer	Output size	Activation function
Sequence input	Feature(2)	-
LSTM	HiddenUnit(100)	-
Fully connected	Class(4)	-
Softmax	Class(4)	Softmax
Classification	-	-

Table 7 Variables used for network training

Variables	Values
Optimizer	Adam
Max epoch	10
Minibatch size	32
Initial learning rate	0.01
Gradient threshold	1
Verbose	False

4. Results and Discussion

4.1 Overall Model Performance

From training the model with 360 sets of dynamic response signal data, divided as shown in **Table 5**, the Recurrent Neural Network (RNN) demonstrated a high overall classification efficiency of 91.67%. The training process was computationally efficient, requiring a total of 9 minutes and 37 seconds to convergence, as shown in **Figure 18**. These results confirm that using axle box acceleration (ABA) data derived from multibody simulation is a viable input for machine learning-based track inspection.

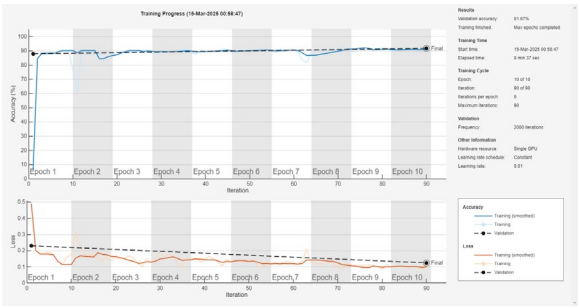

Figure 18 Model performance during training

4.2 Wavelength-Specific Classification Analysis

The prediction results for the three types of isolated defects; short-, medium-, and long-wavelength defects, totaling five locations, with sample defects of each type by wavelength as mentioned in **2.3,** from the 10% testing dataset, can be summarized as follows. **Figures 19–20** show the Predict Activities of testing dataset 16 and 32 respectively, showing the prediction of defect types and locations within signal segments, which are performed implicitly by associating sequence-level classification results with the corresponding spatial positions.

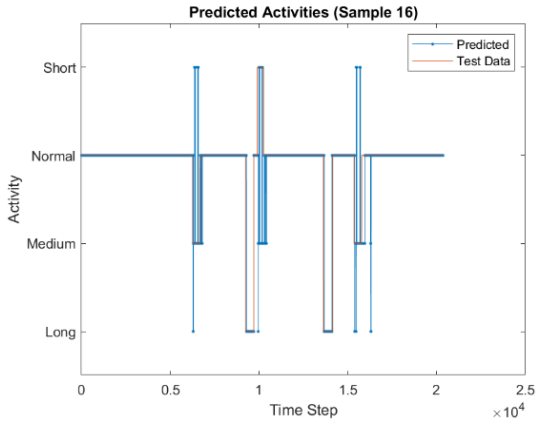

Figure 19 Predict Activities of testing dataset 16

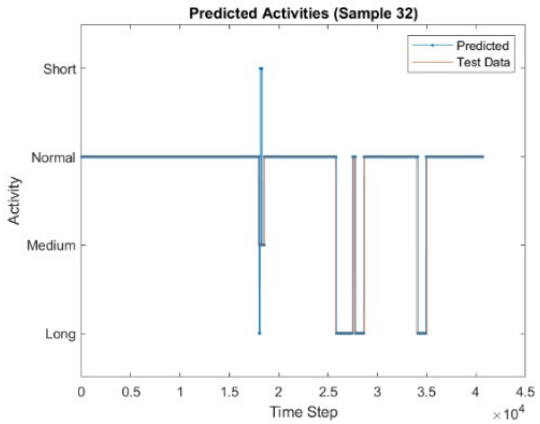

Figure 20 Predict Activities of testing dataset 32

The model's performance varied significantly on the defect types, as evidenced by the confusion matrices for testing datasets 16 and 32 in **Figures 21–22**.

1) **Long-Wavelength Defects:** The model demonstrated robust performance in identifying long-wavelength defects, achieving an F1-score of 0.906 in dataset 16 and 0.928 in dataset 32. This high accuracy suggests that the distinct low-frequency signatures of these defects are well-preserved in the acceleration signal, even at varying speeds.
2) **Medium-Wavelength Defects:** Performance was satisfactory, with F1-scores ranging between 0.792 and 0.844. While recall was acceptable, precision was compromised by occasional misclassification with short-wavelength defects.
3) **Short-Wavelength Defects:** The model faced significant challenges in detecting short-wavelength defects, yielding a low F1-score of 0.204. The confusion matrix reveals a strong tendency to misclassify these defects as medium-wavelength defects or normal track.

Figure 21 Confusion Matrix of testing dataset 16

Figure 22 Confusion Matrix of testing dataset 32

4.3 Critical Analysis of Limitations

The presented results demonstrate the potential of the recurrent neural network model to predict railway track defects efficiently. The model can accurately identify defect locations while effectively classifying defect types, particularly in the case of long-wavelength defects, which yield the most accurate classification results, while medium-wavelength defects achieve satisfactory accuracy levels. For short-wavelength defects, the detection accuracy remains relatively low due to two primary contributing factors:

1) **Speed-Dependent Signal Similarity:** As train speed increases, the duration of the impact from a medium defect shortens, producing a temporal pattern similar to those of short-wavelength defects. Under high-speed conditions (e.g., 120 km/h), the time-domain features of short and medium defects become less separable, confusing the RNN which relies on sequential data patterns.
2) **Random Defect Location Placement:** In this study, defects are randomly distributed along the track, which may cause partial overlap of defect vibration responses in the time domain. This overlap reduces signal separability, particularly for short-wavelength defects, and consequently degrades detection accuracy.

5. Conclusion

This research proposed a railway inspection methodology utilizing a Recurrent Neural Network (RNN) combined with Multibody Simulation (MBS) analysis of axle box acceleration (ABA) signals. The study successfully generated a comprehensive dataset comprising training, validation, and testing sets derived from varying track irregularities and train speeds. The following key conclusions are drawn from the study:

1. **High Overall Efficiency:** The developed RNN model demonstrated strong potential for indirect track monitoring, achieving an average classification accuracy of 91.67% across all defect types. The results confirm that simulated dynamic response data can effectively train neural networks to identify defect locations and types.
2. **Wavelength Sensitivity:** The model proved highly effective in detecting and classifying long-wavelength defects (such as corrugation) and medium-wavelength defects (such as large squats). However, the detection accuracy for short-wavelength defects remained relatively low.
3. **Speed and Model Limitations:** The reduced performance for short defects is primarily attributed to high-speed operating conditions, where the temporal characteristics of short and medium defects become indistinguishable in the time domain. Furthermore, the random placement of defects in the simulation may lead to partial overlap of defect response signal, further reducing signal separability and contributing to misclassification.

Future Work: To overcome these limitations, future research will focus on two main areas. First, advanced signal processing techniques, such as speed-normalized representations or frequency-domain analysis (e.g., wavelet transforms), will be incorporated to improve the discrimination of short-wavelength defects. Second, simulations will adopt a more systematic design of defect placement, with predefined spacing criteria to avoid overlapping response patterns and to promote clearer learning signals for the neural network. Finally, the proposed framework will be validated using real-world axle box acceleration measurements from in-service trains to evaluate robustness under measurement noise and environmental variability.

6. Acknowledgments

This work was financially supported by King Mongkut's Institute of Technology Ladkrabang under Grant number [2566-02-01-058]

7. References

[1] A. Malekjafarian, E. J. Obrien and F. Golpayegani, "Indirect monitoring of critical transport infrastructure: Data analytics and signal processing," in *Data Analytics for Smart Cities*, A. H. Alavi and W. G. Buttlar, Eds., Boca Raton, FL, USA: CRC Press, 2018, ch. 6, pp. 143–157.

[2] A. R. Andrade and P. F. Teixeira, "Unplanned-maintenance needs related to rail track geometry," *Proceedings of the Institution of Civil Engineers - Transport*, vol. 167, no. 6, pp. 400–410, 2014, doi: 10.1680/tran.11.00060.

[3] Z. Wei, A. Núñez, Z. Li and R. Dollevoet, "Evaluating Degradation at Railway Crossing Using Axle Box Acceleration Measurements," *sensors*, vol. 17, no. 10, 2017, Art. no. 2236, doi: 10.3390/s17102236.

[4] W. Fu, Q. He, Q. Feng, J. Li, F. Zheng and B. Zhang, "Recent Advances in Wayside Railway Wheel Flat Detection Techniques: A Review," *sensors*, vol. 23, no. 8, 2023, Art. no. 3916, doi: 10.3390/s23083916.

[5] P. Salvador, V. Naranjo, R. Insa and P. Teixeira, "Axlebox accelerations: Their acquisition and time-frequency characterisation for railway track monitoring purposes," *Measurement*, vol. 82, pp. 301–312, 2016, doi: 10.1016/j.measurement. 2016.01.012.

[6] A. Malekjafarian, E. J. Obrien, P. Quirke and F. Golpayagani, "Railway Track Loss-of-Stiffness Detection Using Bogie Filtered Displacement Data Measured on a Passing Train," *infrastructures*, vol. 6, no. 6, 2021, Art. no. 93, doi: 10.3390/ infrastructures6060093.

[7] E. E. Koks, J. Rozenberg, C. Zorn, M. Tariverdi, M. Vousdoukas, S. A. Fraser, J. W. Hall and S. Hallegatte, "A global multi-hazard risk analysis of road and railway infrastructure assets," *Nature Communications*, vol. 10, 2019, Art. no. 2677, doi: 10.1038/s41467-019-10442-3.

[8] P. Quirke, E. J. Obrien, C. Bowe, D. Cantero and A. Malekjafarian, "The calibration challenge when inferring longitudinal track profile from the inertial response of an in-service train," *Canadian Journal of Civil Engineering*, vol. 49 no.2, pp. 274–288, 2022, doi: 10.1139/cjce-2020-0069.

[9] M. R. Azim and M. Gül, "Damage detection of steel girder railway bridges utilizing operational vibration response," *Structural Control and Health Monitoring*, vol. 26, no. 11, 2019, Art. no. 26:e2447, doi: 10.1002/stc.2447.

[10] Z. Li, M. Molodova, X. Zhao and R. Dollevoet, "Squat treatment by way of minimum action based on early detection to reduce life cycle costs," in *2010 Joint Rail Conference*, Urbana, IL, USA, Apr. 27–29, 2010, pp. 305–311, doi: 10.1115/JRC2010-36184.

[11] Z. Li, R. Dollevoet, M. Molodova and X. Zhao, "Squat Growth—Some observations and the validation of numerical predictions," *Wear*, vol. 271, no. 1–2, pp. 148–157, 2011, doi: 10.1016/j. wear.2010.10.051.

[12] Z. Li, X. Zhao, C. Esveld, R. Dollevoet and M. Molodova, "An investigation into the causes of squats—correlation analysis and numerical modelling," *Wear*, vol. 265, no. 9–10, pp. 1349–1355, 2008, doi: 10.1016/j.wear.2008.02.037.

[13] M. Molodova, L. Zili, A. Núñez and R. Dollevoet, "Automatic Detection of Squats in Railway Infrastructure," *IEEE Transactions on Intelligent Transportation Systems*, vol. 15, no. 5, pp. 1980–1990, 2014, doi: 10.1109/TITS.2014.2307955.

[14] L. Zili, M. Molodova, A. Núñez and R. Dollevoet, "Improvements in Axle Box Acceleration Measurements for the Detection of Light Squats in Railway Infrastructure," *IEEE Transactions on Industrial Electronics*, vol. 62, no. 7, pp. 4385–4397, 2015, doi: 10.1109/TIE.2015.2389761.

[15] Z. Li, M. Oregui, R. Carroll, S. Li and J. Moraal, "Detection of Bolt Tightness of Fish-Plated Joints Using Axle Box Acceleration," in *First International Conference on Railway Technology: Research, Development and Maintenance*, Las Palmas, Spain, Apr. 18–20, 2012, pp. 84, doi: 10.4203/ccp.98.84.

[16] M. Oregui, Z. Li and R. Dollevoet, "Identification of characteristic frequencies of damaged railway tracks using field hammer test measurements," *Mechanical Systems and Signal Processing*, vol. 54–55, pp. 224–242, 2015, doi: 10.1016/j.ymssp. 2014.08.024.

[17] Z. Popović, L. Lazarević, L. Brajović and M. Vilotijević, "The Importance of Rail Inspections in the Urban Area – Aspect of Head Checking Rail Defects," *Procedia Engineering*, vol. 117, pp. 596–608, 2015, doi: 10.1016/j.proeng. 2015.08.220.

[18] M. Molodova, Z. Li and R. Dollevoet, "Axle box acceleration: Measurement and simulation for detection of short track defects," *Wear*, vol. 271, pp. 349–356, 2010, doi: 10.1016/j.wear.2010. 10.003.

[19] S. Suthasupradit, T. Petcharat, K. D. Kim and R. Parichatprecha, "Application of Multibody Dynamics Simulation in Approximation of Rail Vehicle Dynamic Envelope," *Journal of the Korean Society for Railway*, vol. 26, no. 12, pp. 843–855, 2023, doi: 10.7782/jksr.2023.26.12.843.

[20] S. Unsiwilai, W. Phusakulkajorn, C. Shen, A. Zoeteman, R. Dollevoet, A. Núñez and Z. Li, "Enhanced vertical railway track quality index with dynamic responses from moving trains," *Heliyon*, vol. 10, no. 19, 2024, Art. no. e38670, doi: 10.1016/j.heliyon.2024.e38670.

[21] R. Tang, L. D. Donato, N. Bešnović, F. Flammini, R. M. P. Goverde, Z. Lin, R. Liu, T. Tang, V.

Vittorini and Z. Wang, "A literature review of Artificial Intelligence applications in railway systems," *Transportation Research Part C: Emerging Technologies*, vol. 140, 2022, Art. no. 103679.

[22] A. Jamshidi, S. Hajizadech, Z. Su, M. Naeimi, A. Núñez, R. Dollevoet, B. D. Schutter and Z. Li, "A decision support approach for condition-based maintenance of rails based on big data analysis," *Transportation Research Part C: Emerging Technologies*, vol. 95, pp. 185–206, 2018, doi: 10.1016/j.trc.2018.07.007.

[23] A. Malekjafarian, C. A. Sarrabezolles, M. A. Khan and F. Golpayegani, "A Machine-Learning-Based Approach for Railway Track Monitoring Using Acceleration Measured on an In-Service Train," *sensors*, vol. 23, no. 17, 2023, Art. no. 7568, doi: 10.3390/s23177568.

[24] S. Bahamon-Blanco, S. Rapp, Y. Zhang, J. Liu and U. Martin, "Recognition of Track Defects through Measured Acceleration Using A Recurrent Neural Network," *International Journal of Computational Methods and Experimental Measurements*, vol. 8, no. 3, pp. 270–280, 2020, doi: 10.2495/cmem-v8-n3-270-280.

[25] S. Iwnick, "Manchester Benchmarks for Rail Vehicle Simulation," *Vehicle System Dynamic*, vol. 30, no. 3–4, pp. 295–313, 1998, doi: 10.1080/00423119808969454.

[26] A. R. B. Berawi, "Improving Railway Track Maintenance Using Power Spectral Density (PSD)," Ph.D. dissertation, Faculty of Engineering, Univ. Porto, Porto, Portugal, 2013.